International Astronautical Congress, Sydney, Australia, 26 September-3 October 2025.

IAC-25-B1-3-10-x101385

OZFUEL-1: A bushfire risk reduction space telescope

Israel J. Vaughn[a]*, **Joice Mathew**[a], **Tristan Monnier**[a], **Hana Benhizia**[a], **Lu Wang**[a], **Alexey Grigoriev**[a], **Andrew Rakich**[b], **Adam Nagy-Sochacki**[c], **Chris Stokes-Griffin**[c], **Victoria Zinnecker**[c], **John Holmes**[c], **Paul Compston**[c], **Rob Sharp**[a], **Nicolas Younes**[d], **Marta Yebra**[d,e]

[a] *Research School of Astronomy and Astrophysics, The Australian National University* E-mail: israel.vaughn@gmail.com

[b] *KiwiStar Optics* E-mail: my.email@email.com

[c] *New Frontier Technologies, Canberra* E-mail: my.email@email.com

[d] *Fenner School of Environment & Society, The Australian National University* E-mail: marta.yebra@anu.edu.au

[e] *School of Engineering, The Australian National University* E-mail: marta.yebra@anu.edu.au

* Corresponding author

Abstract

Australia has continued to grapple with the impact of increasing frequency and severity of bushfires over the past 2 decades. The "black summer bushfires" of 2019-2020 were particularly devastating in terms of both societal and environmental impacts to Australia. Risk reduction and monitoring of bushfire risk can further enable governments and fire management services to take preventative action to reduce the negative impacts of bushfires on society and the environment. The Australian National University (ANU) is developing a vegetation fuel flammability monitoring space program, OzFuel, which consists of a constellation of small satellites assessing wavelengths in the ShortWave InfraRed (SWIR). OzFuel-1 is a technology demonstrator sensor under development as a step in the larger OzFuel program. OzFuel-1 is a multispectral small satellite sensor collecting 4 wavebands in the SWIR. We present the optical design, the opto-mechanical design, the dimensionally stable carbon fibre composite optical mounting option developed by New Frontier Technologies Pty Ltd, and the planned environmental tests to achieve TRL 5-6 to map the bushfire fuel loads. At SWIR wavelengths, thermal emission from spacecraft structure which contaminates the reflected light from the forest canopy can compromise the data integrity if not carefully managed. The OzFuel-1 payload will use the Leonardo SAPHIRA eAPD detector. The payload design maintains a contrast of greater than 50% at the Nyquist frequency of the detector. The OzFuel-1 telescope is a modified Richter-Slevogt catadioptric design followed by an optical relay and a cooled pupil stop to manage the thermal emission contamination from spacecraft structure and warm optics. The optical system past the cool stop is held to a temperature less than $\lesssim -20^\circ$ C. The system is compact with a length of about 300 mm to the focal plane. The optical elements have been designed to survive launch loads whilst maintaining the required performance. A successful OzFuel-1 program will demonstrate the feasibility of medium-resolution SWIR sensor for bushfire fuel load monitoring, paving the way for the full OzFuel constellation. This capability has the potential to significantly enhance Australia's fire risk assessment and management strategies, contributing to improved early warning systems and more effective mitigation of bushfire impacts.

Nomenclature

We describe the various symbols and physical quantities used in this article in this section.

Symbol	Description	Notes
L	Radiance	in $\frac{W}{\text{mm}^2\ \text{sr}}$ or $\frac{\text{photons}}{\text{mm}^2\ \text{sr}\ s}$
E	Irradiance	in $\frac{W}{\text{mm}^2}$ or $\frac{\text{photons}}{\text{mm}^2\ s}$
sr	Solid angle units	steradians

Acronyms/Abbreviations

Acronym	Description
AITC	Advanced Instrumentation and Technology Centre
AIVT	assembly, integration, verification, and test
ANU	Australian National University
BRCoE	Bushfire Research Centre of Excellence
ConOps	concept of operations
CTE	coefficient of thermal expansion
CRC	Cooperative Research Centre
eAPD	electron avalanche photo-diode
FFOV	full field of view
GSD	ground sampling distance
MTF	modulation transfer function
NFT	New Frontier Technologies
e^-	photo-electron
PSF	point spread function
SNR	signal to noise ratio
SRD	spatial resolution distance
SWIR	short wave infrared
TOA	top of atmosphere
TBAL	Thermal balance
TRL	Technology Readiness Level
TVAC	Thermal vacuum

1. Introduction

The BRCoE at the ANU, in collaboration with various partners, has been developing the OzFuel program since 2018. The program seeks to develop a constellation of satellites and associated research, concepts, and payloads to monitor bushfire fuel flammability in the Australian context. The program initially focuses on the development of science and technology to derive flammability metrics for bushfire risk monitoring for eucalypt forests to be expanded to other critical fuel types into the future [1–3]. As part of this program, OzFuel-1, a technology demonstrator sensor, has been conceived to validate the program concept and has been aligned to the OzFuel Phase A report [4]. The program is broad, and includes development of optical payload, detector, and mechanical technologies. Extensive detector work is also being undertaken for the program [5,6].

The science drivers for the program are primarily outlined in the Phase A report [4] with specifics about the wavelength selection in the calibration report for SmartSat CRC [7]. We present 1) the novel optical design, requirements, and sensitivity analyses 2) novel carbon fibre mechanical design elements for optical element fixturing, and 3) the test plan and performance validation plans to qualify the optical elements to TRL5-6.

1.1 Optical Payload Requirements

OzFuel-1 will adapt the ANU Rosella control electronics for the SAPHIRA eAPD infrared detector manufactured by Leonardo. The detector has low read noise and is sensitive at the wavelengths required for the OzFuel payloads [8–10]. The detector characteristics are outlined in Table 1.

Table 1: Leonardo eAPD array general parameters.

Parameter	Description
Size	320 X 256 and 512 X 512 pixels
Pixel size	24 μm
Wavelength range	$\sim 800 - 3500$ nm depending on gain
Read noise	~ 9 e^- at at unity gain and 80 K
Dark current	< 0.1 e^-/s at a unity gain and 80 K
Conversion	~ 4.2 e^-/ADU at unity gain
Full well	$\sim 275,000$ e^- at unity gain

The Phase A study [4] determined that the GSD should be $50 - 60$ m. Note that due to Nyquist this implies that the SRD is $= 100 - 120$ m. Using 50 m as the GSD requirement drives the focal length of the optical system to be 264 mm for the Leonardo pixel size assuming an orbit of 550 km. This determines the pixel crossing time to be 7.15 ms given the orbital height and the ground velocity of $6,994$ m/s at that height. Along track SRD could be improved by reducing the exposure time. The complete optical requirements are shown in Table 2, and we explain the detail and justification in the following sections.

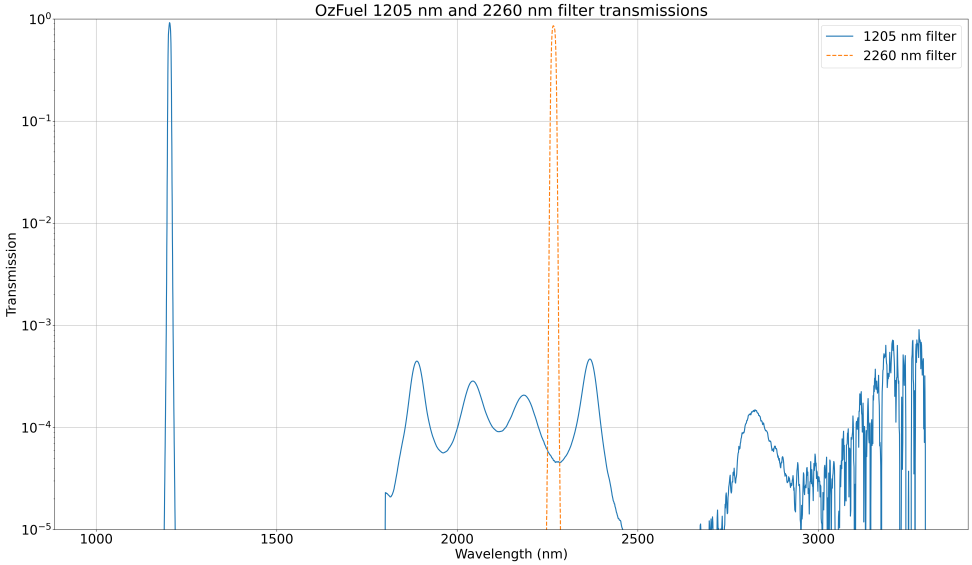

Fig. 1: The 1205 nm and 2260 nm filter transmission profiles. Log scaled. Provided by Alluxa.

Table 2: Optical design requirements. Note the different FFOVs for different detector models.

Requirement	Description
Focal length	264 mm
Exposure time	< 7.2 ms
Focal ratio	2.6
FFOV SAPHIRA	9.8 mm at the focal plane, 20.49 km on the ground, 2.13 deg.
FFOV 512 X 512	17.4 mm at the focal plane, 36.20 km on the ground, 3.77 deg.
MTF contrast	$> 50\%$ at 20.83 cycles/mm at detector, 10 cycles/km at the ground
Throughput	$> 40\%$ from $\lambda = 1205 - 2260$ nm
Wavelengths	1205 nm, 1660 nm, 2100 nm, 2260 nm
Bandpass	10 nm
SNR	>= 100

The optical design was developed in collaboration with KiwiStar Optics and manufactured by KiwiStar. We also present our summarised integration plan in this article.

1.2 Mechanical design

The OzFuel-1 project has taken a dual-pronged mechanical design approach, developing a standard aluminium fixturing design alongside a new space appropriate carbon fibre structure with tailored CTE behaviour designed and manufactured by New Frontier Technologies Pty Ltd. This approach allows for innovation while reducing risk to the qualification of the OzFuel-1 optics.

1.3 Testing and verification

The OzFuel-1 optical design will be function and performance tested in the lab under nominal operating conditions, including cool stop and mechanical structure cooling simulating in orbit conditions. We present our test and validation plan in this article.

2. Optical design

The optical design began from the requirements and utilised past knowledge generated from a previous infrared space telescope design at ANU. The aperture and throughput for the SNR requirement are analysed, as well as thermal background contributions. Note that the design process is and was iterative, and went through multiple iterations before being finalised as presented here.

2.1 Spectral Filters

We have selected the wavelengths of interest for the OzFuel program as shown in Table 2 derived from analsyis of data from a field campaign [7]. We have procured the 1205 nm and 2260 nm filters from Alluxa. The filter profiles are shown in Figure 1. The filters consist of a band-

pass filter on the second surface, and a broader out of band blocking filter on the first surface. The physical filters are shown in Figure 2

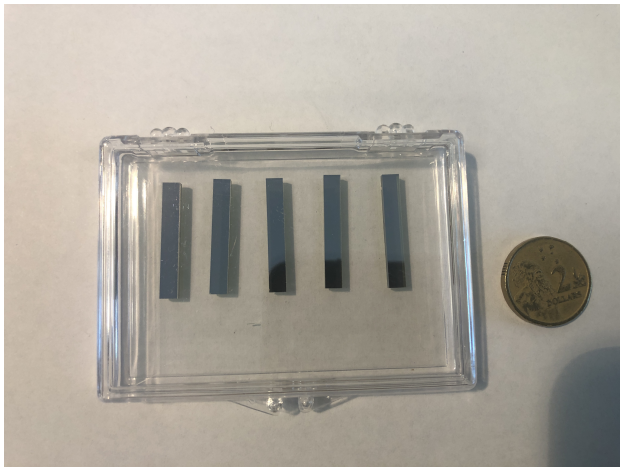

Fig. 2: Alluxa filters for 1205 nm and 2260 nm.

2.2 *Sensitivity*

The albedo of eucalypt forest is $\sim 5-10\%$ in the SWIR landsat bands of 1609 nm and 2200 nm [11]. We use these bands as a reference for the OzFuel-1 sensitivity estimates as they are close in wavelength to our selected wavelength bands. We use the ASTM G173 standard solar spectrum to estimate radiometry and SNR. We use an albedo of 5% and 10% for the 1205 nm and 2260 nm bands and denote these "eucalypt low albedo" and "eucalypt high albedo" resepctively. For this analysis, we are shot noise limited. The read noise and dark current are, however, included. We assume that the Earth surface temperature is 300 K and also that the front lens element is at 300 K. We assume that the structure and cool stop are at 253 K. We assume a telescope overall transmission of 40%, and the optical parameters as specified in Table 2.

The full well capacity of Leonardo detectors is low at high gains. To achieve the low noise provided by the high gains, the detector must be kept below saturation. Radiometric analysis indicates that for a 7.2 ms exposure time the 1205 nm band pixels will receive $\sim 240,000$ e^- for the desert land type (typically the brightest type that will be seen by the sensor) and $\sim 60,000$ e^- for the high range of the eucalpyt land type. This leads to two scenarios, one where we set integration times to accomodate the desert land type, or one where we set integration times based on the eucalypt radiometry and accept saturation viewing brighter land types. The Leonardo uses 16-bit digitisation, implying that we require 3.66 e^-/ADU for the desert and 0.92 e^-/ADU for the high range of eucalypt, or somewhere in between the two. This corresponds to gains of ~ 1.2 and ~ 4.6 respectively for the Rosella system. The dark current from Leonardo detectors is low for gains up to ~ 5 at ~ 0.025 e^-/s/pixel [12]. At the relevant integration times for the OzFuel-1 payload, the dark current is negligible compared with the number of photo-electrons in the signal. The read noise at unity gain is $\sim 9e^-$, and about $\sim 0.5e^-$ for a gain of 30. The largest impact from read noise will be on the SNR for the low brightness eucalypt signal at 2260 nm, that contains $\sim 18,000e^-$ per pixel for the 7.2 ms exposure time. The reduction in SNR for this signal for a read noise of 9 e^- versus 0.5 e^- is about 0.3%. These analyses assume the worst case read noise of 9 e^-.

Detector parameters (e.g. quantum efficiency) are incorporated into the analysis. We also present generic desert and tree scenes sourced from ECOSTRESS [13].

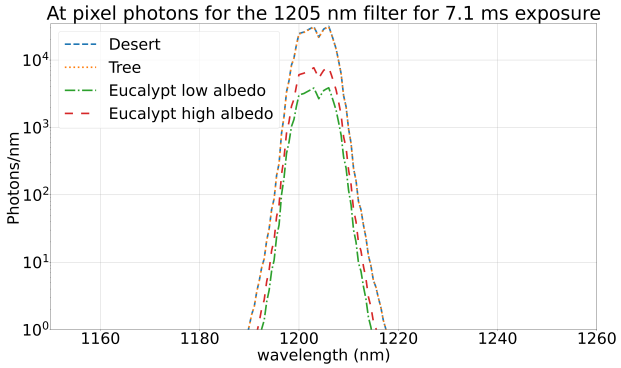

Fig. 3: At pixel fluxes for the 1205 nm filter for a variety of land types. Log scaled.

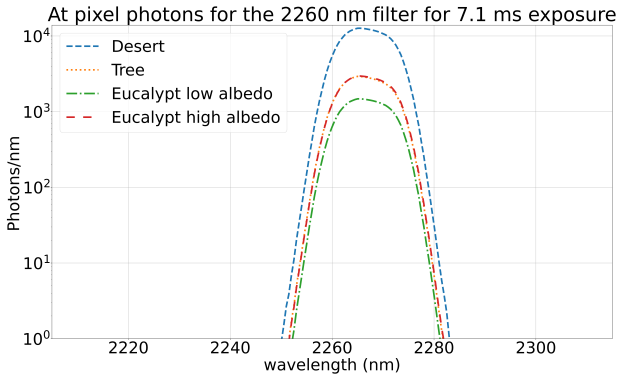

Fig. 4: At pixel fluxes for the 2260 nm filter for a variety of land types. Log scaled.

Figures 3 and 4 show the spectrally resolved fluxes for a pixel given the optical parameters and the filter profiles specified. The total flux at the pixel is computed by integration over the entire spectrum for each filter. The total fluxes are shown in Table 3.

Table 3: Estimated total fluxes for a variety of land types at the pixel for the OzFuel telescope. Desert and tree types use spectrally resolved albedo derived from ECOSTRESS data [13] and the eucalypt albedos are derived from CSIRO analysis [11].

Land type	Total Flux/pixel	Spectral filter
desert	$2.4e5$ e^-	1205 nm
desert	$1.6e5$ e^-	2260 nm
tree	$2.4e5$ e^-	1205 nm
tree	$3.6e4$ e^-	2260 nm
eucalypt low	$3.0e4$ e^-	1205 nm
eucalypt low	$1.8e4$ e^-	2260 nm
eucalypt high	$6.0e4$ e^-	1205 nm
eucalypt high	$3.6e4$ e^-	2260 nm
Earth thermal emission	3.6 e^-	1205 nm
Earth thermal emission	22.0 e^-	2260 nm
Foreoptics thermal emission at 300K	32 e^-	1205 nm
Foreoptics thermal emission at 300K	50 e^-	2260 nm
Structure thermal emission at 253K	124 e^-	1205 nm
Structure thermal emission at 253K	64 e^-	2260 nm
Structure thermal emission at 300K	$2.0e3$ e^-	1205 nm
Structure thermal emission at 300K	$3.2e3$ e^-	2260 nm
Structure thermal emission at 330K	$8.0e3$ e^-	1205 nm
Structure thermal emission at 330K	$2.2e4$ e^-	2260 nm

SNR calculations utilise the spectrally resolved at pixel fluxes. The centre of each band with a 20 nm full bandpass is extracted, integrated over the 20 nm band and used as the signal. The remaining photons, which include the out of band leakage, are used as background. Also included in the background is the Earth thermal emission, and thermal emission from the front elements at a temperature of 300 K, the structure thermal emission at 253 K, the detector dark current, and the detector read noise.

Table 4: Estimated SNR for a variety of land types at the pixel for the OzFuel telescope with the cool stop and structure set to 253 K (-20° C).

Land type	SNR	Spectral filter
desert	490	1205 nm
desert	276	2260 nm
tree	490	1205 nm
tree	189	2260 nm
eucalypt low	171	1205 nm
eucalypt low	135	2260 nm
eucalypt high	243	1205 nm
eucalypt high	189	2260 nm

Table 4 shows the final estimated SNR numbers for a variety of land types. Note that we meet the requirement for eucalypt to have an SNR of greater than 100. The impact of thermal structure background is significant as shown

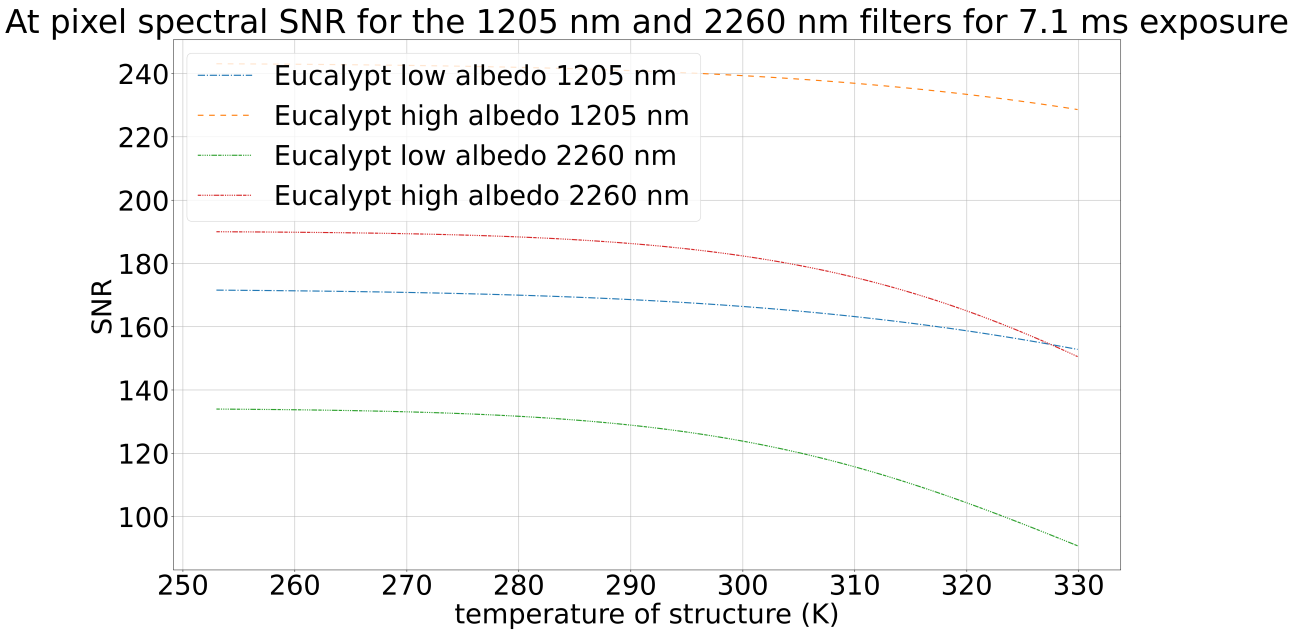

Fig. 5: SNR curves versus the thermal emission from the optical structure for the low and high eucalypt land types for 1205 nm and 2260 nm band filters.

in Table 3 and Figure 5, especially for temperatures over 300 K. The thermal emission from the structure for the 2260 nm band is shown in Figure 6. The background contribution as a percentage of the signal at 300 K is $\sim 7\%$ in the 1205 nm band for the low eucalypt albedo, and $\sim 17\%$ in the 2260 nm band. Using a cool stop and cooling the structure to $-20°$ *C* significantly reduces the thermal background, to $\sim 0.4\%$ and $\sim 0.3\%$ respectively. It also reduces the risk of thermal variation and hot satellite bus environments. At $\sim 50°$ *C* the thermal background from the structure rises to $\sim 27\%$ and $\sim 120\%$ of the signal for the 1205 nm band and 2260 nm band respectively. These large variations in thermal background over temperature range can significantly impact the bushfire risk estimates. The cool stop and controlled thermal structrure design mitigates this risk.

2.3 Reflective vs Catadioptric

A fully reflective set of fore-optics for the telescope were considered early on in the design phase of the telescope. A primary driver for using a catadioptric design was the potential to build upon prior work completed in our instrumentation program; a diffraction limited catadioptric design using 3 elements and fully spherical surfaces. The spherical catadioptric design has the potential to positively impact the cost and effort for manufacturing and AIVT.

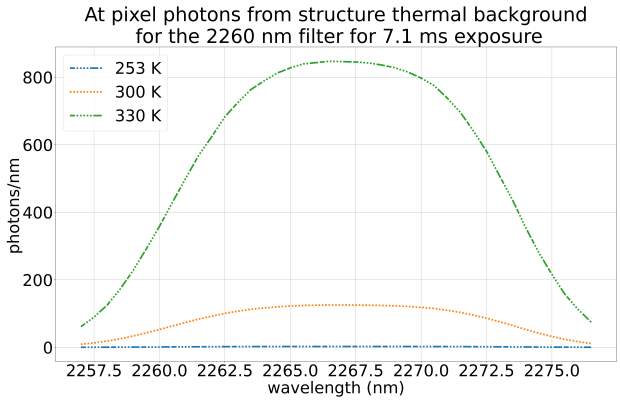

Fig. 6: Thermal emission from the structure for 253 K, 300 K, and 330 K for the 2260 nm band filter.

The tradeoff is that a refractive foreoptic design may have more transmission losses than a reflective design. We analyse the tradeoff briefly in this section.

We assume that a refractive design has anti-reflective coatings with 99% transmission and that the foreoptics refractive elements are 25 mm thick and made of Corning HPFS7979 fused silica. HPFS7979 has better than 99.7% transmission per 10 mm for the wavelengths required for

OzFuel-1. Protected silver has a reflectivity of about 98% across the OzFuel wavelengths. Protected gold is also feasible, with similar reflectivities to silver for the OzFuel-1 wavelengths. We assume a central obscuration with the same size for both a reflective and refractive design of 50%. A two element reflective telescope with no refractive correctors would require complex aspheres with precise positioning for an $f/2.6$ system. Mitigation of this complexity can be accomplished by corrector elements after the reflective elements. Corrected reflector designs are included in the analysis shown in Table 5. Corrector elements are assumed to have a thickness of 10 mm.

Table 5: transmissions and complexity for a variety of telescope designs. rfr denotes refractive elements, rfl denotes reflective elements, corr denotes corretor elements, t is the transmission for that design, c denotes the complexity of manufacturing and AIVT for the design, and cata. denotes a catadioptric design. The selected design is highlighted in green.

Type	# rfr	# rfl	# corr	t	c
Fully reflective	0	2	0	0.48	very high
Fully reflective	0	3	0	0.47	high
Fully reflective	0	4	0	0.46	high
Reflective corr.	0	2	2	0.46	medium-high
Reflective corr.	0	3	2	0.45	medium-high
Reflective corr.	0	2	3	0.45	medium
OzFuel cata.	3	2	0	0.45	low-medium

The decrease in transmission from the best possible design for transmission, a 2 element reflector, to the selected catadioptric design, is about $\sim 8\%$. Given the SNR calculations in the previous section, the reduction of risk and complexity of using an already developed design form, and the ease of manufacture and AIVT for all spherical elements, we chose the catadioptric foreoptics design form for the OzFuel telescope.

2.4 Image quality

A standard rule of thumb for imaging systems is for the MTF curve to be at greater than 50% contrast at the Nyquist frequency of the detector for reasonable imaging performance. The detector specified has 24 μm pixels which implies that the Nyquist frequency is 20.833 cycles/mm (equivalent 10 cycles/km on the ground). Contrast reversal is also an unwanted effect (when the optical transfer function passes through zero or the MTF is zero). A rule of thumb to keep this from occurring is to place a constraint of $10-20\%$ contrast requirement at double the Nyquist frequency.

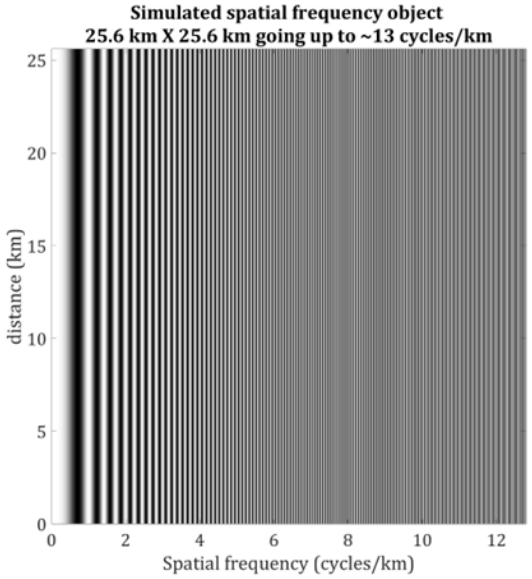

Fig. 7: Resolution target used for the MTF simulation.

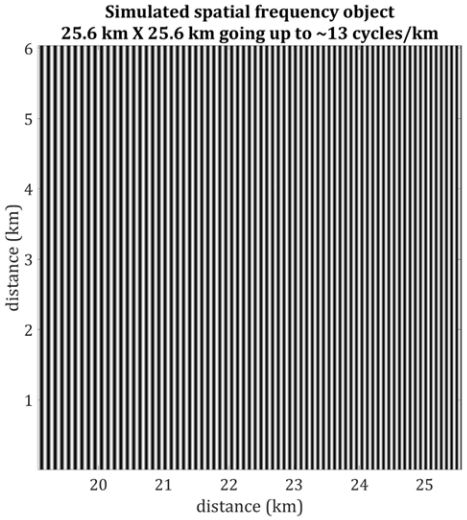

Fig. 8: Zoomed in view of the right hand side of the resolution target used for the MTF simulation showing up to 13 cycles/km.

Ideally we would want contrast to remain high until the Nyquist frequency, with a low pass optical filter and a sharp cutoff just beyond Nyquist, but most lens/telescope designs cannot accommodate this.

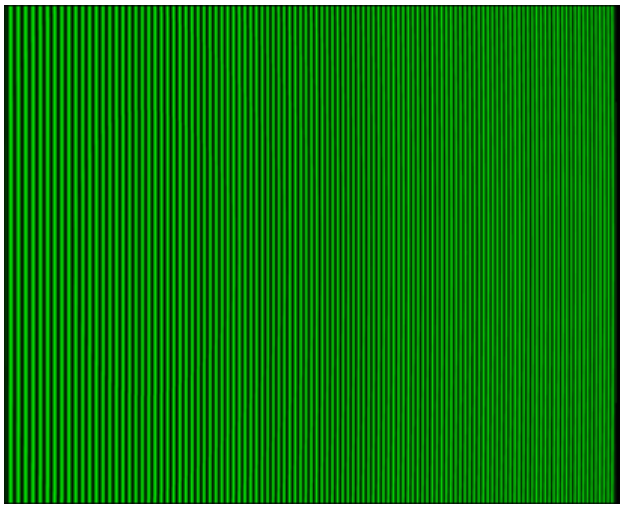

Fig. 9: Zoomed in view of the right hand side of the resolution target imaged with the OzFuel telescope at $f/2.6$ for 2260 nm. Note the good contrast.

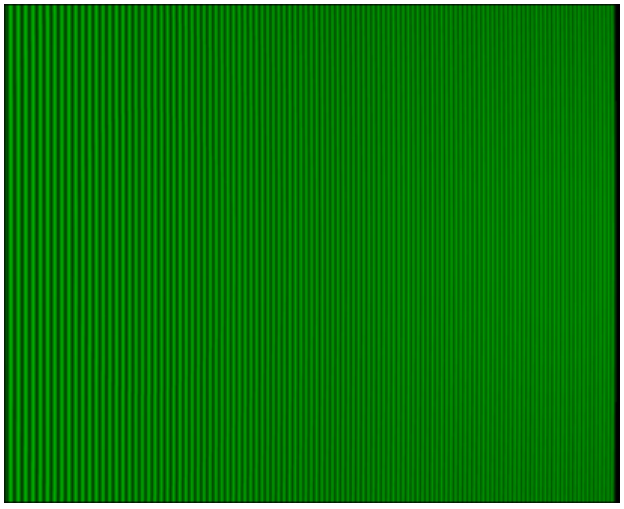

Fig. 10: Zoomed in view of the right hand side of the resolution target imaged with the OzFuel telescope at $f/4.0$ for 2260 nm. Note the significant reduction in contrast.

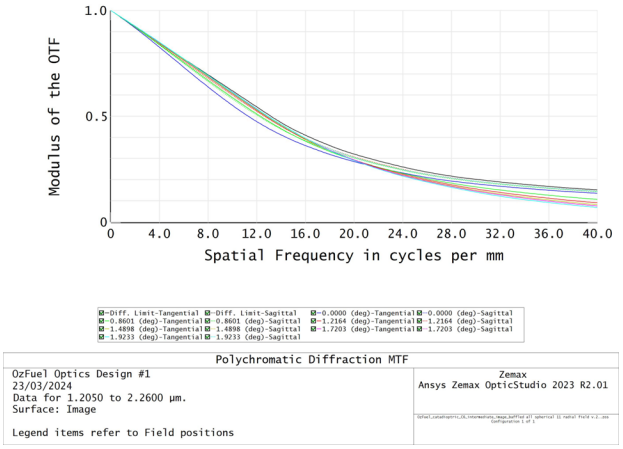

Fig. 11: MTF curve for the OzFuel telescope at $f/4.0$. Note the contrast of 30% at the Nyquist frequency.

Figure 7 shows a simulated resolution target that we use to show the MTF effects. This target goes a little beyond Nyquist at with the rightmost part of the target having a spatial frequency of 13 cycles/km on the ground as shown in Figure 8.

The imaging system must provide enough contrast for features to be discernible in the measured images, and "good performance" corresponds to better than 50% contrast at the Nyquist cutoff frequency of the detector. Figures 9 and 10 show the f/2.6 system (required to meet the "good performance" requirement) versus an f/4.0 system. The figures show resolution targets with spatial frequencies near the Nyquist limit. Figure 11 shows that the f/4.0 system has about 30% contrast at the detector Nyquist frequency. Additionally, the faster telescope will provide a better SNR.

2.5 Design

The foreoptics design is a modified Richter-Slevogt catadioptric design iterating on previous design forms developed by the optical instrumentation group at ANU. KiwiStar optics improved and modified the design, in collaboration with the OzFuel team.

The design abides by the "d/6" rule for the optical element diameter to thickness for robustness and launch load and vibration survival. The design was restricted to a length of 300 mm to ensure a reasonable footprint for a small satellite payload. The 3 foreoptics elements and L6-L8 are made from Corning HPFS 7979, L4 is S-LAH98, L5 is S-LAH99, and L9 is S-NPH3. L3 is a Mangin mirror with a hole cut in the centre, and the second surface of L2

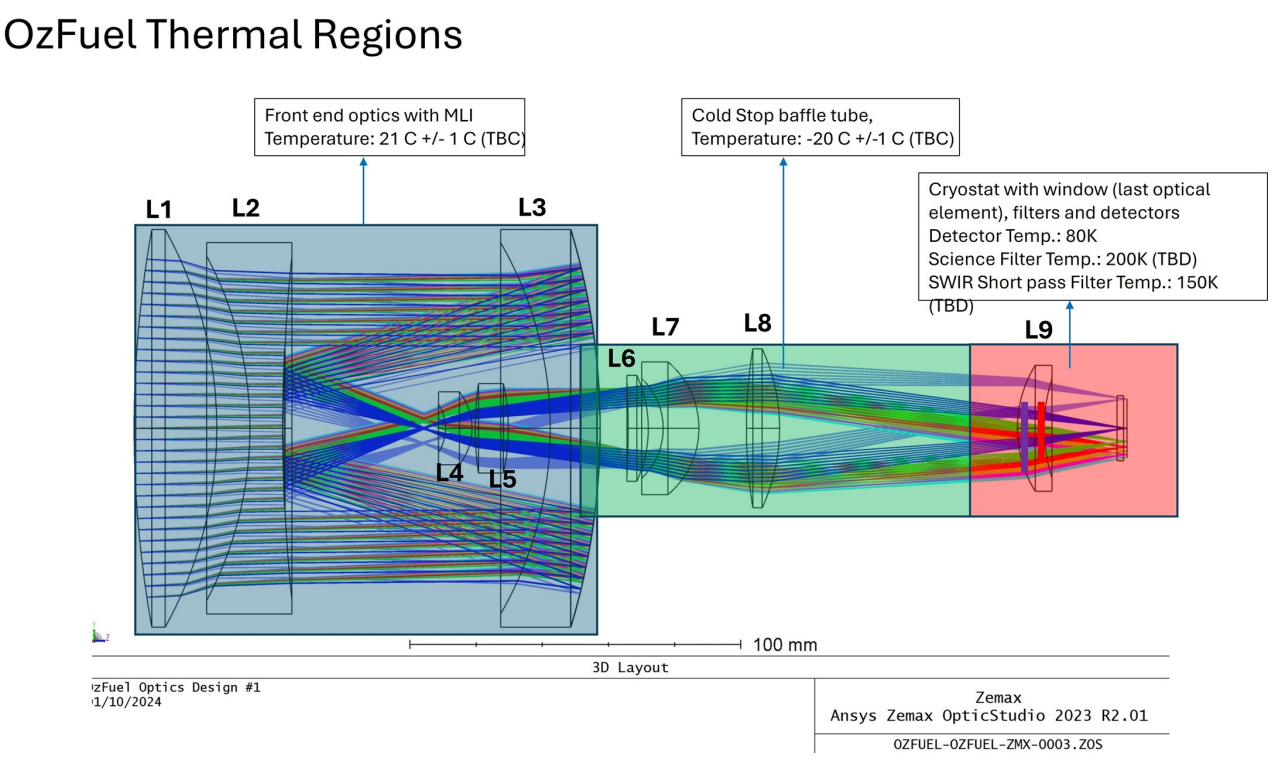

Fig. 12: OzFuel-1 telescope optical design layout, including annotated temperature zones. The 3 element foroptics form an image between the second and third element. Elements 4-9 relay the image and form an intermediate pupil plane where a cool stop is placed. The pupil plane is at the front of element 6.

has a spot mirror coated on the surface. Both are coated with protective silver. The Alluxa filters are placed on a 2 mm substrate in front of the detector with a 1 mm gap. The foreoptics are compact, with a length of 140 mm, and the entire system is 300 mm in length including the relay optics. The nominal MTF has a contrast of $> 60\%$ at the Nyquist frequency, shown in Figure 13.

The design consists of 3 lens groups, L1-L3 in a large tube (group 1), L4-5 (group 2), and L6-L8 (group 3), with L9 being used as the cryostat window for the detector cryostat.

The telescope incorporates a cool pupil stop at L6 to control thermal radiation from the structure. All structure and optics past L6 need to be held at a lower temperature compared with the group 1 and group 2 optics. L9 will also need to be held at the same temperature as the group 3 optics. The analysis in Section 2.2 suggests that a temperature of ~ 250 K is sufficient.

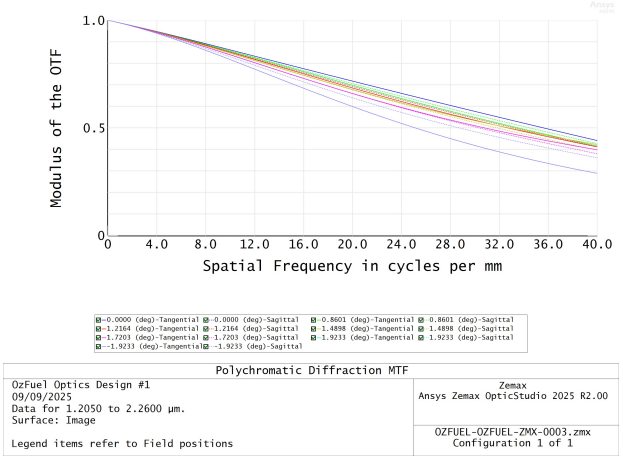

Fig. 13: Nominal MTF curves for the OzFuel-1 design.

3. Mechanical design

3.1 Design drivers

The mechanical design must ensure that the elements remain within the optical tolerances, that the elements are alignable using standard integration procedures, that the elements are athermalised for a valid operational temperature range, and that the system is mountable for AIVT. Radially athermalised mounting techniques [14, 15] are utilised for all elements. An additional design driver for this project was the use of a cryostat for AIVT. The detector used for lab functional and performance testing necessarily must be housed in a cryostat due to the 80 K operational temperature, and this requires the last element of the optical train to be used as the cryostat window, see Section 3.4.

3.2 Aluminium design

Traditional mounting techniques with facility for alignment have been used for both the aluminium and carbon fibre (discussed in the following subsection) structure designs. The designs incorporate silicone encapsulated elements in an alignable spring and washer configuration. The springs provide force during the alignment process, and once aligned the elements are fixed in place using a silicone adhesive. The silicone adhesive is space qualified with a CTE selected to radially athermalise the optical elements across the element CTEs and the CTE of aluminium. The gaps between the element and the structure wall is then set using the DeLuzio athermalisation technique [14].

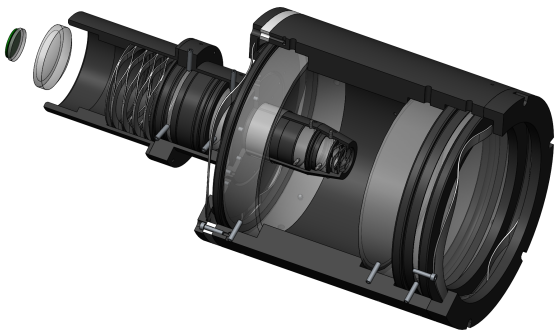

Fig. 14: Traditional aluminium structure design.

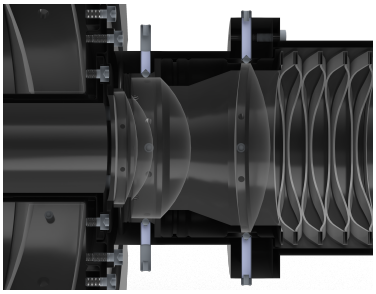

Fig. 15: Traditional aluminium structure design detail of 3rd lens group. The radial alignment screws shown will be removed after adhesive is cured.

3.3 Carbon fibre design

The OzFuel program has partnered with NFT to design and manufacture a dimensionally stable composite mount Figure 16. For this application, a near-zero axial coefficient of thermal expansion (CTE) was required, while the radial CTE needed to be tuned to enable effective athermalisation using a three-material design approach [14]. The laminate consisting of 92 plies was optimised in three independent sections for the stepped geometry (Figure 17) before candidate laminates were coupled together for a low CTE system. A near-zero axial CTE of -0.15×10-6 K-1 was achieved between lenses L1 to L3 and L2 to L3, the lenses with the greatest spacing. The radial CTE varies at each lens location and is a byproduct of the low CTE axial laminate. For all the low axial CTE laminate candidates investigated only a corresponding subset of radial CTE values can be used. Given the subset of achievable radial CTEs and the possible gap dimensions for adhesive based on composite ply thickness increments, an athermalisation model was used to select the combination that minimises gross dimensional movement of the lenses. Axial movement over a 100 degree temperature increase is show in Figure 18. The mount was finally manufactured from a space-qualified, low-outgassing CF/PEEK composite using laser-assisted automated fibre placement.

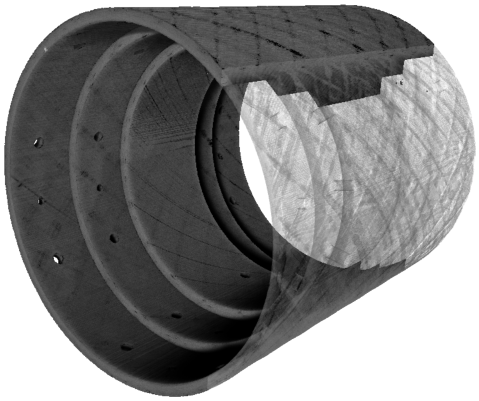

Fig. 16: Novel carbon fibre tube structure.

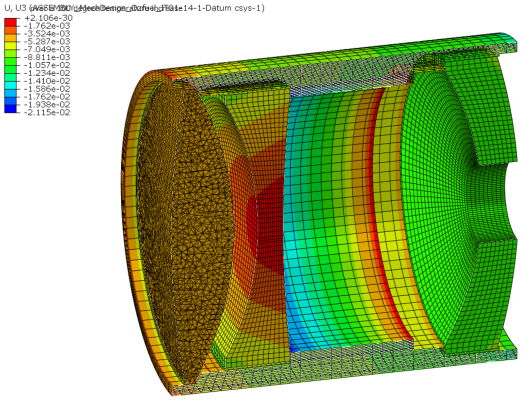

Fig. 17: Section view of the NFT structure with lens.

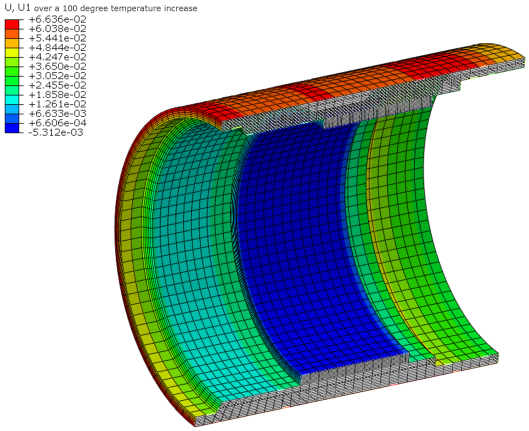

Fig. 18: Axial movement of the carbon fibre structure over 100 degree temperature range.

3.4 Cryostat

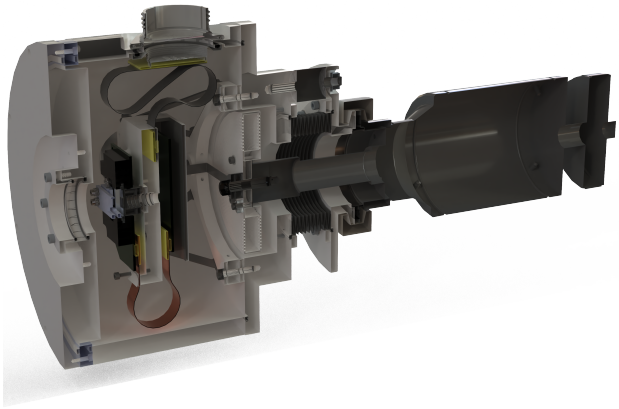

Fig. 19: Cryostat section view.

For lab testing, the Leonardo detector must be cooled. A concurrent detector control system development program, Rosella [6, 16], is providing control for the Leonardo detector. The OzFuel-1 program will use this existing equipment, with some modifications, to test the OzFuel-1 optical telescope (Figure 19).

3.5 Filter mounting

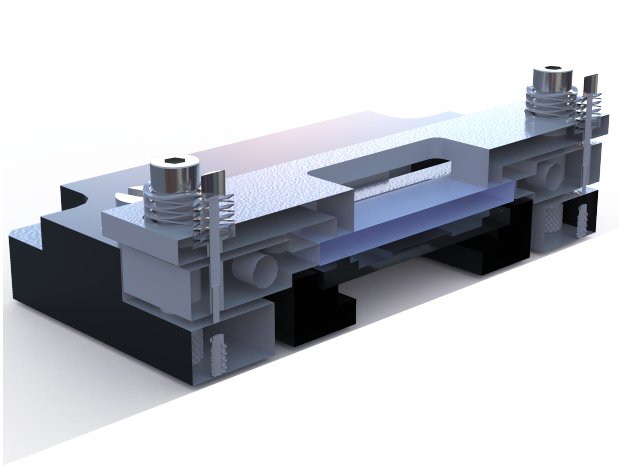

Fig. 20: Filter mount section view.

The Alluxa spectral filters must be mounted 1 mm in front of the focal plane, and this must be done in the existing cryostat and detector mounting scheme. Each filter is 25 mm × 3.748 mm × 2 mm (width × height × thickness).

The filter mounting scheme uses a spring loaded mechanism to sandwich the filters between FR-4 circuit board material (which is suitable for vacuum environments), shown in Figure 20.

4. Performance testing plan

The OzFuel-1 optical system will be tested for performance under appropriate thermal conditions using standard MTF performance measurement techniques with the Imatest™ software suite and a suitable collimator and resolution target shown in Figure 21. The outcomes will validate the optical design thermal performance to TRL5-6. TRL 5 is defined as "Laboratory Testing of Integrated/Semi-integrated System: System Component and/or process validation is achieved in a relevant environment." TRL 6 is defined as "Prototype System Verified: System/process prototype demonstration in an operational environment (beta prototype system level)" [17].

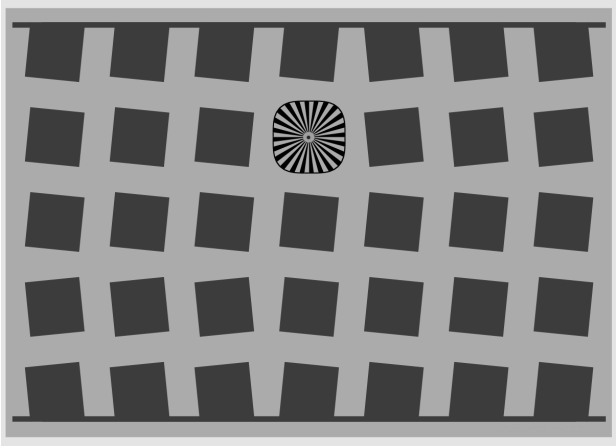

Fig. 21: Resolution target used to feed the collimator.

The optical elements from KiwiStar are on schedule to be completed mid-September of 2025. After receipt by the ANU instrumentation team, AIVT will commence, after which the Suite #1 set of performance and validation tests will be performed as shown in Table 6. These tests are expected to be completed by the end of 2025. This will result in the optics being validated to TRL 6 for thermal operation, and TRL 5 for the entire system including the detector. Subsequent tests are planned for a future effort to reach TRL 7 as described in Table 7. These tests are planned in the Wombat XL space environment chamber located in the AITC at Mt. Stromlo observatory.

Table 6: Suite #1: Thermal and operational tests for optical system.

Test	Description	Test ID
MTF at thermal operation conditions	Validates MTF requirement	1.1
MTF at thermal operation conditions after thermal cycling	Validates MTF requirement under satellite thermal variance conditions	1.2
MTF at room temperature	Taken with the above tests, bounds performance varation under representative thermal variation	1.3
Optical throughput	Validates throughput requirement	1.4

Table 7: Suite #2: Space environment tests for optical system.

Test	Description	Test ID
Vibration and post vibration MTF measurement for GEVS	Validates launch survival	2.1
Space environment TBAL and TVAC and post MTF measurement	Validates MTF requirement under space environment thermal and vacuum conditions	2.2
In situ space environment MTF test	Validates telescope MTF performance under operating conditions in the space environment	2.3

4.1 Test setup

The testing and validation setup for test Suite #1 must provide the correct thermal environment, allow for light to be propagated into the telescope, and allow for the cryostat and detector to be aligned to the main telescope body. We utilise an existing large cryostat with modifications to provide the necessary thermal environment. The initial tests will cool the telescope structure to 253 K (-20° *C*), and can be cooled further if the tests show that thermal contam-

ination is too large at that temperature. The cryostat has an existing thermally controlled platen which can be used to cool the relevant telescope structure. Modifications have been made to the large cryostat to enable dry, dehumidified gas to flow around the cold telescope structure and optics to prevent condensation. The detector cryostat sits externally, and can be adjusted to attain focus and centration with the OzFuel-1 telescope assembly.

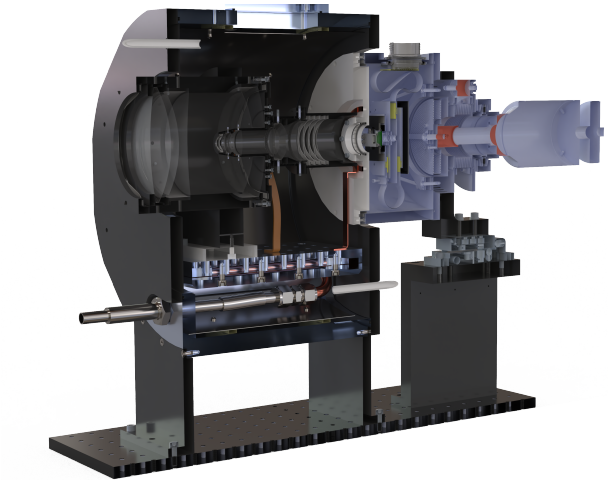

Fig. 22: Section view of the test setup for OzFuel-1 performance testing. The enclosing cryostat with thermal platen surrounds the telescope structure.

5. Discussion and conclusions

The OzFuel-1 technology demonstrator sensor is underway to reach TRL5-6 by the end of the year. Simulated radiometry indicates that the telescope design conforms to the science goals and requirements. By the end of 2025 our testing will validate the design performance under expected thermal operating conditions and also confirm that the cool stop rejects thermal background adequately.

Next steps include finalising and analysing 1660 nm and 2100 nm filter designs, the securing additional funding to progress the pathfinder to TRL 7+, and building a space qualified payload. Together, these efforts establish a clear pathway from lab design to in-orbit demonstration, laying the foundation for a space-based capability to reduce bushfire risk and support ecosystem management.

Acknowledgements

This work was funded by the SmartSat CRC (projects P3-24 and P8-02), whose activities are funded by the Australian Government's CRC Program and by CRC-P grant CRCPXV000005

References

[1] N. Younes, M. Yebra, J. Mathew, and R. Sharp, ''Ozfuel: a space-based vegetation fuel flammability monitoring system,'' in *Sensors, Systems, and Next-Generation Satellites XXVII*, vol. 12729, pp. 367–372, SPIE, 2023.

[2] N. Younes, M. Yebra, and D. Hughes, ''Ozfuel phase a–spectral database report,'' tech. rep., 2023.

[3] N. Younes, M. Yebra, M. M. Boer, A. Griebel, and R. H. Nolan, ''A review of leaf-level flammability traits in eucalypt trees,'' *Fire*, vol. 7, no. 6, p. 183, 2024.

[4] T. Errabih, A. Grigoriev, A. Vaccarella, B. Taylor, D. Chandler, I. Vaughn, J. Gilbert, J. Ward, J. U. Lee, J. Mathew, *et al.*, ''Ozfuel phase a study report: Space-based australian forest fuel flammability monitoring,'' 2022.

[5] J. Mathew, J. Gilbert, R. Sharp, A. Grigoriev, S. King, A. Vaccarella, D. Chandler, N. Herrald, I. Price, and A. Magniez, ''A space-based near-infrared sky survey to study the oxygen abundance in cool stars,'' in *Space Telescopes and Instrumentation 2020: Optical, Infrared, and Millimeter Wave*, vol. 11443, pp. 78–90, SPIE, 2020.

[6] J. Mathew, J. Gilbert, R. Sharp, A. Grigoriev, N. Cardena, and M. Yebra, ''Infrared remote sensing using low noise avalanche photodiode detector,'' *arXiv preprint arXiv:2210.04770*, 2022.

[7] N. Younes and M. Yebra, ''Pre-launch ozfuel preliminary cal/val technical report,'' 2023.

[8] G. Finger, I. Baker, D. Alvarez, C. Dupuy, D. Ives, M. Meyer, L. Mehrgan, J. Stegmeier, and H. J. Weller, ''Sub-electron read noise and millisecond full-frame readout with the near infrared eapd array saphira,'' in *Adaptive Optics Systems V*, vol. 9909, pp. 354–373, SPIE, 2016.

[9] D. Atkinson, D. Hall, S. Jacobson, and I. M. Baker, ''Photon-counting properties of saphira apd arrays,'' *The Astronomical Journal*, vol. 155, no. 5, p. 220, 2018.

[10] K. Lake, V. Isgar, I. Baker, M. Herrington, L. Hipwood, C. Maxey, H. Weller, K. Barnes, and M. Hicks, ''Developments in the saphira family of hgcdte apd infrared arrays for low flux sensing: present and

future,'' in *Sensors, Systems, and Next-Generation Satellites XXIV*, vol. 11530, pp. 76–85, SPIE, 2020.

[11] I. Lau, C. Ong, Y. Guo, M. Caccetta, G. Squire, and R. Woodcock, ''Landsat 8 continental analysis of australia,'' Data Collection v1, CSIRO, 2023.

[12] D. E. Atkinson, D. N. Hall, S. M. Jacobson, and I. M. Baker, ''Dark current in the saphira series of apd arrays,'' *The Astronomical Journal*, vol. 154, no. 6, p. 265, 2017.

[13] J. B. Fisher, B. Lee, A. J. Purdy, G. H. Halverson, M. B. Dohlen, K. Cawse-Nicholson, A. Wang, R. G. Anderson, B. Aragon, M. A. Arain, *et al.*, ''Ecostress: Nasa's next generation mission to measure evapotranspiration from the international space station,'' *Water Resources Research*, vol. 56, no. 4, p. e2019WR026058, 2020.

[14] J. J. Herbert, ''Techniques for deriving optimal bondlines for athermal bonded mounts,'' in *Current Developments in Lens Design and Optical Engineering VII*, vol. 6288, pp. 180–190, SPIE, 2006.

[15] P. R. Yoder, *Mounting optics in optical instruments*, vol. 181. SPIE press, 2008.

[16] J. Gilbert, A. Grigoriev, S. King, J. Mathew, R. Sharp, and A. Vaccarella, ''Linear-mode avalanche photodiode arrays for low-noise near-infrared imaging in space,'' *arXiv preprint arXiv:1911.04684*, 2019.

[17] Defence Science and Technology Group (Australia), ''Technology readiness level definitions and descriptions,'' tech. rep., Defence Science and Technology Group, Australia, n.d. Technical note; no specific author indicated.